Send Orders for Reprints to reprints@benthamscience.ae

Temperature Dependence of the Optical Band Gap and Optical Parameters of Tetramethyl Ammonium Tetrachlorozincate $(TMA)_2ZnCl_4$ single Crystals Around the Normal and Incommensurate Phase Transitions

A. Abu El-Fadl* and A.M. Nashaat

Physics Department, Faculty of Science, Assiut University, Assiut, 71516, Egypt

Abstract; Single crystals of tetramethylammonium tetrachlorozincate $[N(CH_3)_4]_2ZnCl_4$ abbreviated hereafter as $(TMA)_2ZnCl_4$ were grown using the slow evaporation technique at 315 K. The X-ray powder diffraction patterns indicated that $[N(CH_3)_4]_2ZnCl_4$ belongs to the orthorhombic system with *Pmcn* symmetry at room temperature. The lattice constants are found to be a= 12.360 Å, b= 15.687 Å and c= 8.985 Å. The values were in good agreement with the values in previous studies. Ultraviolet–visible–near-infrared (UV–Vis–NIR) spectral studies were carried out in the temperature range 276–307 K. This range of temperature involves two phase transition temperatures (T_i=296 K) from normal (parent) to incommensurate phase and (T_c=279 K) from incommensurate to commensurate-ferroelectric phase. The cut off wavelength was found to be 195.016 nm at room temperature. The optical transmittance increases with increasing temperature, and the cut off shifts to higher wavelengths. Analysis reveals that the type of optical transition is the indirect allowed one. The optical energy gap (E_g) has the value of 5.903 eV at room temperature. The value of optical energy gap (E_g) decreases with increasing temperature. The changes in the values of the cut off wavelength and optical energy gap (E_g) with changing the temperature were found to take different rates at the two phases under study, besides anomalous takes place at T_i and T_c. The absorption coefficient (α) as a function of the incident photon energy shows an exponential behavior near the absorption edge which suggests that the Urbach rule is obeyed and indicated the formation of a band tail. Urbach parameters were calculated at different temperatures and the frequencies of effective phonons and electron–phonon interaction constants were determined for various phases.

Keywords: $(TMA)_2ZnCl_4$ single crystals, Crystallization, Optical characterization, Temperature dependence of band gap, Urbach rule.

1. INTRODUCTION

The A_2BX_4 type crystals (with A=K, NH_4, Rb; B=Zn, Co, Mn, Cu; X=Cl, Br, I) have been interested because of their incommensurately modulated structures and the successive phase transitions. Most of these materials exhibit many physical properties related to ferroelectric and commensurate or incommensurate phase transitions [1-2]. A_2BX_4 crystal family shows many physical properties related to structural phase transitions at low temperatures. These fundamental properties make this crystal family suitable for several applications such as temperature and humidity sensors [1], and memory effects that manifest themselves as temperature anomalies in their physical properties [3]. Tetramethylammonium tetrachlorozincate $(TMA)_2ZnCl_4$ crystal has turned out to be a very interesting member belong to a A_2BX_4, undergoes different phase transitions at and below room temperature. Under atmospheric pressure, the transition temperatures are 296 K, 280 K, 276.4 K, 182 K and 91 K. The highest temperature phase (parent or paraelectric phase, PE) belongs to the *Pmcn* symmetry. In this phase, a unit cell contains four formula units [3]. Among these transitions, a study of the C-IC transition (T_c) has attracted more attention because of interesting physical phenomena in its phase transition such as an abnormal polarization-electric field (P-E) hysteresis loop at temperatures near T_c. At temperatures slightly above T_c, the material consists of locally commensurate regions separated by a domain wall called a discommensuration (DC) of a phase solition, where the modulation and the phase of an order parameter change abruptly. It has been believed that DCs play a decisive role in the C-IC transition [4].

Theoretical and experimental investigations were carried out on $(TMA)_2ZnCl_4$ crystals for their variety of phase transitions. Anomalous changes of the spontaneous polarization, the coercive field, and the spectrum of the distribution of polarization relaxation times are detected in $(TMA)_2ZnCl_4$ at uniaxial pressures in the range where a transition arises to a nonuniform state with several coexisting waves of structural modulation by Gladkii and Kirikov [5]. On the other hand, Lim and Jung [6] studied phase transformations in these crystals by proton magnetic resonance. Structural phase transition in TMA-compounds was carried out through thermal expansion measurements by Wiesner *et al.* [7]. The crystal structure in VI phase was reported by Curtiss *et al.* [8]. Dielectric relaxation was investigated by Hong *et al.* [9] and

*Address correspondence to this author at the Physics Department, Faculty of Science, Assiut University, 71516 Assiut, Egypt; Tel: +20882412135; E-mail: abulfadla@yahoo.com

1874-088X /15

birefringence studies were conducted by Sveleba *et al.* [10] and Vlokh *et al.* [11].

The previous optical studies on the NLO materials draw little attention in terms of temperature dependence of the optical properties. Therefore, the present work is devoted to study the crystallization and the effect of temperature on the optical properties of $(TMA)_2ZnCl_4$ single crystal in a range of temperatures that involves two phase transition temperatures T_c (commensurate-incommensurate phase transition) and T_i (incommensurate-paraelectric phase transition).

2. EXPERIMENTAL PROCEDURE

2.1. Synthesis and Crystal Growth

Tetramethylammonium tetrachlorozincate was synthesized using tetramethylammonium chloride ($C_4H_{12}NCl$) and Zinc chloride ($ZnCl_2$) as starting materials. Salts of the starting materials were mixed in aqueous solution using double distilled water as a solvent in a stoichiometric ratio given by the following equation:

$$2(C_4H_{12}NCl) + ZnCl_2 \rightarrow [N(CH_3)_4]_2\ ZnCl_4 \quad (1)$$

The synthesized material was subjected to repeat recrystallization by dissolving the crystallized salt in double distilled water and the recrystallization occur by the natural evaporation of the solution, this process was repeated several times for purification. The filtered clear solution was kept in a constant temperature bath of high accuracy. Good quality transparent seed crystals were obtained by spontaneous nucleation in 10 days. Single crystals of $(TMA)_2ZnCl_4$ were grown by slow evaporation of the saturated solution at pH= 4, and at constant temperature (315 K) by using an indigenous crystal growth apparatus fabricated in our laboratory. The solution was saturated at the growth temperature (315 K) by slow evaporation or by lowering temperature gradually from higher temperature to this temperature. Small seed was suspended in the saturated solution using a nylon thread from a stirrer, which was rotated with speed of 20 rpm. Care was taken to minimize thermal variations and mechanical disturbances.

2.2. Powder X-ray Diffraction Measurements

For X-ray diffraction measurements, a sample from the crystal was grated very well until it became fine powder then small amount from this powder was taken to be used in these measurements. X-ray powder diffraction pattern was recorded using a Philips PW 1710 diffractometer. The measurements were swapped from $2\theta = 4°$ to $2\theta = 60°$ with step of 0.06°, copper target at 40 kV, 30 mA, a scanning speed of 0.06°/min and incident wavelength $\lambda_{K\alpha}$= 1.5418 Å.

2.3. Optical Measurements

The grown crystal was cut into thin rectangular plates about 1 mm in thickness and 20 mm^2 in area to be used for optical measurements. The prepared plates were transparent and clear from any noticeable defects. The optical transmittance was measured by using Shimadzu UV–VIS-2101 PC dual-beam scanning spectrophotometer with un-polarized monochromatic light in the range 190–900 nm. The temperature of the sample was controlled using an ultra-thermostat (Mgw Lauda type K2R, Germany) and it was measured with an accuracy of $\pm$0.1 K. The optical transmittance was measured for the specimen for several times at different temperatures ranging from 272 to 307 K with step of 1 K.

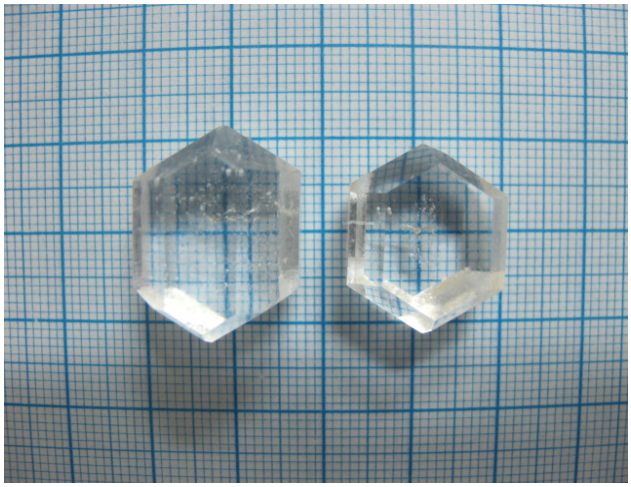

Fig. (1). Photograph of as grown $(TMA)_2ZnCl_4$ single crystals.

3. RESULTS AND DISCUSSION

3.1. Crystal Growth and Structural Analysis

Single crystals of $(TMA)_2ZnCl_4$ were grown by isothermal evaporation method. After 50 days, a highly transparent and well faceted good quality, optically transparent, large size single crystals with the dimension of 25 × 15 × 8 mm^3 were obtained as shown in Fig. (**1**).

The X-ray powder diffraction pattern collected at room temperature is presented and the diffraction peaks were indexed in Fig. (**2**). It is seen from the XRD pattern that the sharp peaks indicate the good crystallinity of the crystal. The $(TMA)_2ZnCl_4$ crystallizes in the orthorhombic system with the space group *Pmcn*, and the unit cell parameters refined by the least square method and labeled according to international standards ($c < a < b$). These values are in good agreement with the values reported in the literature and close to the average value of the parameters obtained for the $(TMA)_2ZnCl_4$ [7, 12] as shown in Table **1**.

3.2. Absorption Coefficient

The absorption coefficient (α) can be calculated using the relation:

$$\alpha = \frac{2.303}{t}\log(\frac{1}{T}) \quad (2)$$

Where T_λ is the spectral transmittance and t the sample thickness.

The absorption coefficient (α) calculated using equation (2) is represented versus the photon energy ($h\nu$) for

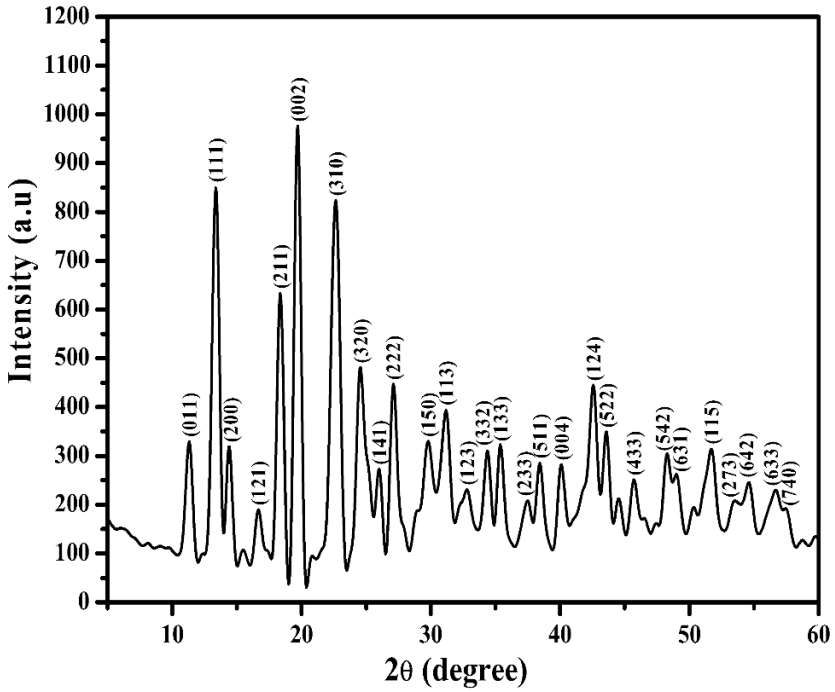

Fig. (2). Room temperature powder XRD patterns of $(TMA)_2ZnCl_4$ crystals.

Table 1. Values of the lattice constants a (Å), b (Å) and c (Å) of $(TMA)_2ZnCl_4$.

a, b, c Values			
Determined	**Reported**		
	[7]	[12]	PDF 05-001-0024
a= 12.360 Å	a= 12.276 Å	a= 12.268 Å	a= 12.258 Å
b= 15.687 Å	b= 15.541 Å	b= 15.515 Å	b= 15.503 Å
c= 8.985 Å	c= 8.998 Å	c= 8.946 Å	c= 8.987 Å

$(TMA)_2ZnCl_4$ single crystals at different temperatures in Fig. (**3**). The general trend of α is the continuous increasing with increasing hν, above the absorption edge α increases more rapidly with hν. At different crystal temperatures the α – hν dependence varies, as the figure shows that the magnitude of α decreases with increasing temperature. Near the transition temperatures the dependence tends to take a different shape near the absorption edge.

3.3. Optical Transition

The optical band gap (E_g) was determined from the measured optical data using the following equation:

$$\alpha = \frac{B(h\nu - E_g)^n}{h\nu} \quad (3)$$

Where α is the optical absorbance, B is a constant depends on the nature of the material, hν is the incident photon energy in eV, E_g is the optical band gap and n is a constant describes the nature of the optical transition between the valence and conduction bands. By plotting $(\alpha h\nu)^{1/2}$, $(\alpha h\nu)^{1/3}$, $(\alpha h\nu)^2$ and $(\alpha h\nu)^{2/3}$ versus photon energy (hν) at different values of n; and select the optimum linear part. Equation (3) can be used to reveal the type of the optical transition. It is found that for $(\alpha h\nu)^{1/2}$ the relation yields linear dependence, which indicate the type of the optical transition for this crystal is an allowed indirect transition; then E_g value can be determined by extrapolating the linear portion to α=0. As shown in Fig. (**4**), the plot was analyzed using the above equation. The values of the optical energy gap E_g determined from Fig. (**4**), is represented in Fig. (**5-i**). Fig. (**5-ii**) depicts the relation between cut off wavelength and photon energy (hν). The cut off wavelength increases with increasing crystal temperature and two anomalies appear at the phase transitions temperatures T_i and T_c. Values of the optical energy gap (E_g) and the cut off wavelength at selected temperatures are listed in Table **2**. Fig. (**5-i**) shows that the indirect energy gap decreases with increasing temperature. For example, it shifts from 6.005 to

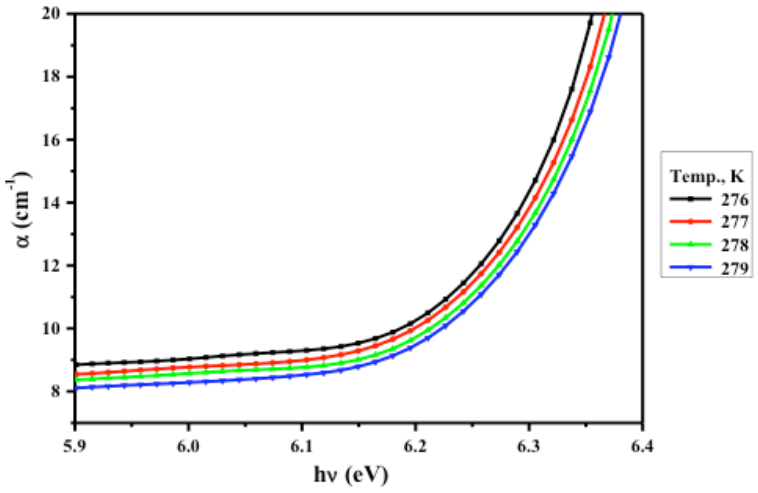

(**i**)

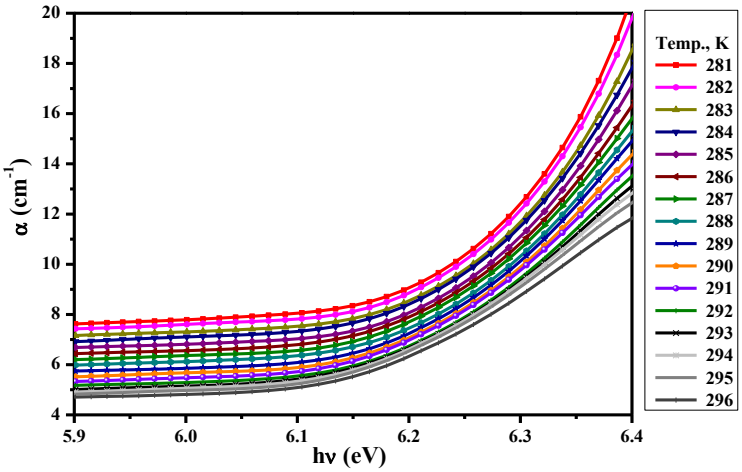

(**ii**)

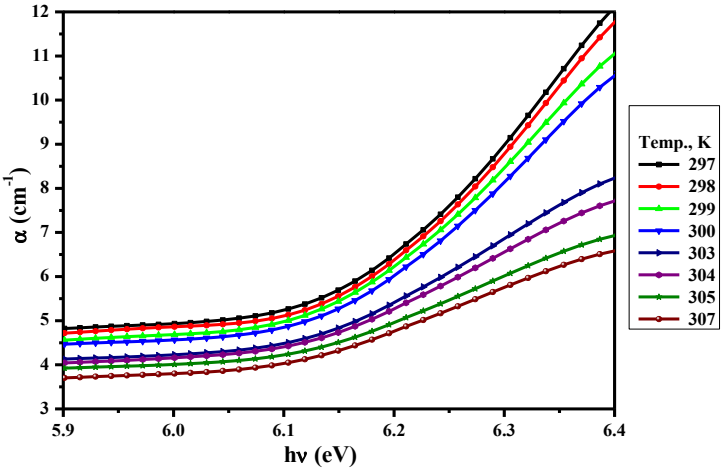

(**iii**)

Fig. (3). The absorption coefficient α versus photon energy (hν) at different temperatures (**i**) around the commensurate ferroelectric (CF) region, (**ii**) around the incommensurate (C) region and (**iii**) around the normal paraelectric (N) region for $(TMA)_2ZnCl_4$ single crystal.

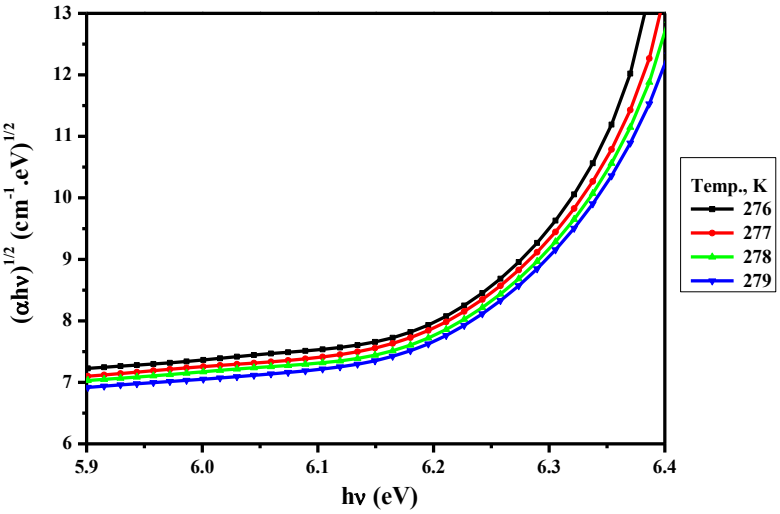

(**i**)

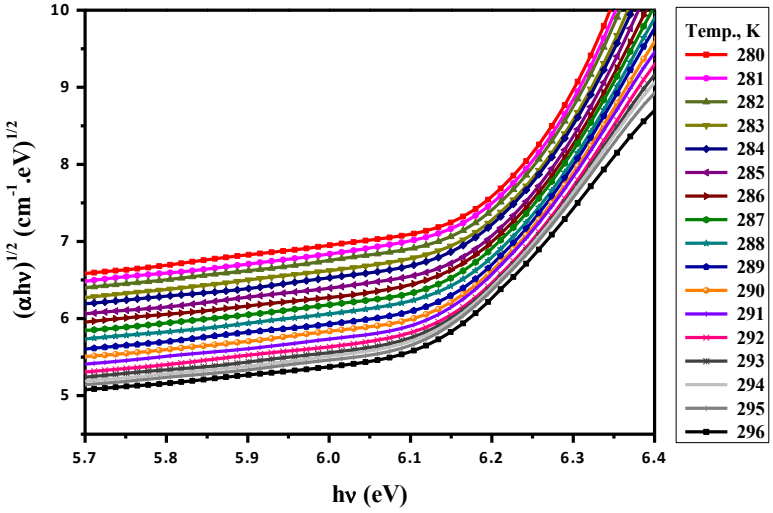

(**ii**)

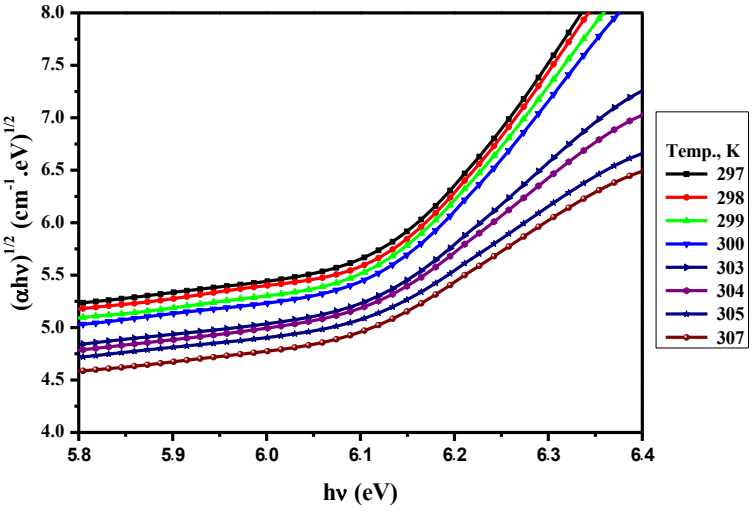

(**iii**)

Fig. (4). $(\alpha h\nu)^{1/2}$ versus photon energy (hν) at different temperatures for $(TMA)_2ZnCl_4$ single crystal (**i**) around the commensurate ferroelectric (CF) region, (**ii**) around the incommensurate (C) region and (**iii**) around the normal paraelectric (N) region.

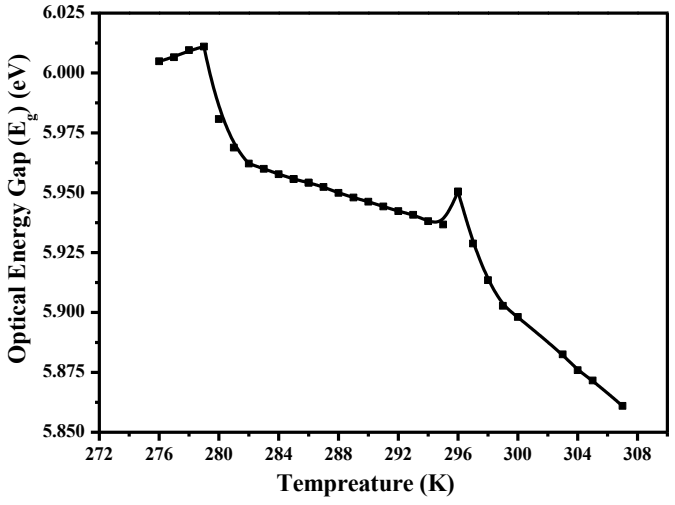

(**i**)

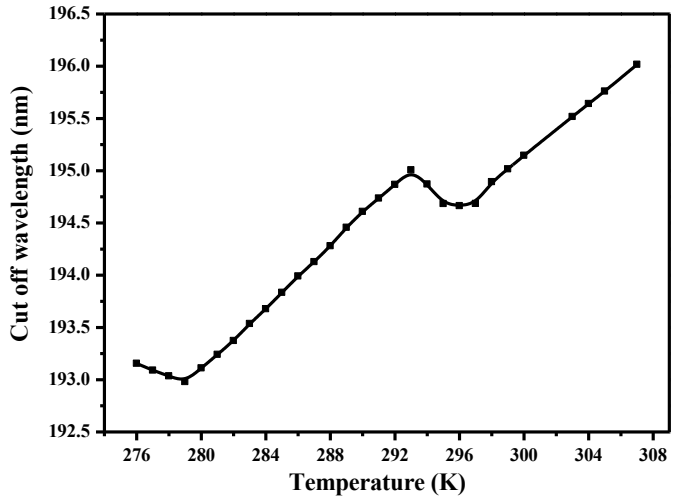

(**ii**)

Fig. (5). (**i**) The optical energy gap (E_g) dependence on temperature (**ii**) the Cut off wavelength for $(TMA)_2ZnCl_4$ single crystals dependence on temperatures.

Table 2. The cut off wavelength, optical energy gap (E_g), Urbach tail energy (E_e) and the steepness parameter (σ) at selected temperatures for $(TMA)_2ZnCl_4$ single crystals.

Temperature (K)	Optical Energy Gap E_g (eV)	Cut off Wavelength (nm)	Urbach Tail Energy E_e (eV)	Steepness Parameter $\sigma \times 10^3$
276	6.005	193.155	0.9002	52.839
279	6.011	192.980	0.8839	54.401
283	5.960	193.535	0.6405	76.143
289	5.948	194.457	0.6798	73.273
296	5.950	194.663	0.7373	69.191
303	5.882	195.517	0.5443	95.938
307	5.861	196.017	0.5614	94.244

Table 3. Values of phonon frequency and electron-optical-phonon parameters for $(TMA)_2ZnCl_4$ crystal near the normal (PE or N), incommensurate (IC) and commensurate (CF) phases.

Phase	E_o (eV)	ln α_o	α_o (cm^{-1})	σ_o	ν_o (THz)	g
CF	6.274	2.632	13.895	0.1213	14.981	5.496
IC	6.149	2.127	8.3906	-0.1234	26.331	-5.402
PE or N	5.818	1.091	2.9760	-0.0514	37.093	-12.97

5.861 eV as the temperature increases from 276 to 307 K and the decreasing rate becomes faster where anomalies take place at normal (N)-Incommensurate (IC), T_i and incommensurate (IC)-commensurate (ferroelectric) (CF) phase transition temperature T_c. Same observations are reported in Abu El-Fadl *et al.* [13] study of the dielectric permittivity (ε) temperature dependence along the three crystallographic directions. ε-T relationship exhibit peak values at the normal (N)-incommensurate (IC) (T_i=296 K) and incommensurate-commensurate (ferroelectric) (CF) (T_c=279 K) phase transitions. In this study, the d.c and a.c electrical conductivity measurements showed anomalous variations at the same transition temperatures. In the other hand, the temperature dependence of the optical birefringence obtained by Sveleba *et al.* [14] for $[N(CH_3)_4]_2ZnCl_4$ crystals pure and doped with Ni^{2+}, indicated that, the commensurate–incommensurate transition is accompanied by an inflection in the curves, which is indicative of the presence of continuous phase transition. It was also suggested in [14] that the rotations of all tetrahedral groups are correlated near T_i in the parent phase. It was also noted that, the intensity of quasi-elastic neutron scattering in the parent phase increases sharply when approaching the parent–incommensurate phase transition point (T_i) [15].

Our results confirm the results reported earlier [13] with respect to the anomaly occurred in T_i phase which is higher than that in T_c phase, and attributed to the domain walls and to the onset of the free rotation of $ZnCl_4^{2-}$ ions at the transition temperatures.

The value of E_g for $(TMA)_2ZnCl_4$ crystal at room temperature (299 K) is 5.903 eV (Table **2**). This value is very close to the value of 5.89 eV calculated by El- Korashy [16] for the direct band gap energy at 300 K (the normal paraelectric phase) for this crystal. On the other hand, the calculated E_g values for $(TMA)_2ZnCl_4$ crystal is greater than those for $(TMA)_2CoCl_4$ and $(TMA)_2MnCl_4$ [17]. The estimated values lies between 4.553 and 4.667 eV for $(TMA)_2CoCl_4$ and between 5.351 and 5.383 eV for $(TMA)_2MnCl_4$ crystals.

3.4. Urbach Rule

The absorption coefficient dependence on the incident photon energy could be described satisfactorily by an exponential behavior at the absorption edge. At different temperatures the relation between the absorption coefficient (α) with the photon energy (hν) is given by Martienssen [18] who modified Urbach's rule [19], to take the form:

$$\frac{\alpha}{\alpha_O} = \exp\left[\sigma \Big/ \left\{kT\left(h\nu - h\nu_\circ\right)\right\}\right] \quad (4)$$

Where α_o and $h\nu_o$ are constants [20] depend on the characteristic of the crystal, hν is the incident photon energy, σ is the steepness parameter, a temperature dependent parameter which characterizes the broadening of the absorption edge [21]. Simple mathematical treatment of equation (4) makes the equation to take the form of linear dependence. In fact, a relation between Ln(α) and hν at certain constant temperature should yield a straight line and a family of straight lines could be obtained at different temperatures between 276 and 307 K which confirms the exponential dependence of the absorption coefficient (α) on the energy of the incoming photon (hν) as required by Urbach's rule (Fig. **6**). The straight lines, treated by the least squares method, converge to point with coordinates α_o and $h\nu_o$ called "converging point". Table **3**, contains the values of α_o and $h\nu_o$ for $(TMA)_2ZnCl_4$ crystals at selected temperatures covering the measured temperature range. The values of E_o and α_o decrease with increasing crystal temperature. The effect is more pronounced in case of values calculated at transition temperatures.

Urbach's rule describes the broadening of the absorption edge and the formation of a band tail, thus another parameter, known as Urbach tail energy (E_e) which should be inversely proportional to σ, is introduced to describe the width of the tails due to localized states in the absorption edge [20]:

$$E_e = \frac{k_B T}{\sigma} \quad (5)$$

Using Equation (5) where the value of σ at each temperature was calculated from the slope of the associated straight line in Fig. (**6**), the Urbach tail energy (E_e) is calculated at different temperatures. The obtained values are listed in Table **2**. It has been found that the Urbach tail energy (E_e) decreases with increasing crystal temperature. More important, (E_e) and the optical energy gap (E_g) both exhibit two anomalies at the same temperatures 279 K and 296 K which corresponds to the crystal phase transitions T_c and T_i respectively (Fig. **7-i**; Table **2**).

3.5. Broadening of the Absorption Edge

In ionic crystals, the equation relating the steepness parameter (σ) with the crystal temperature and photon energy can be written in the form [22]:

$$\sigma(T) = \sigma_o \frac{2k_B T}{h\nu_o} \tanh \frac{h\nu_o}{2k_B T} \quad (6)$$

Where $h\nu_o$ is the energy of the optical phonons interacting with the optical transitions, σ_o is a temperature-independent but material-dependent parameter being inverse-

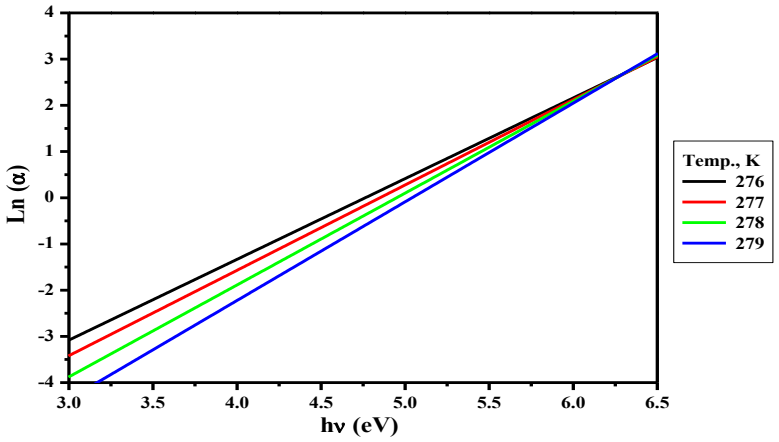

(**i**)

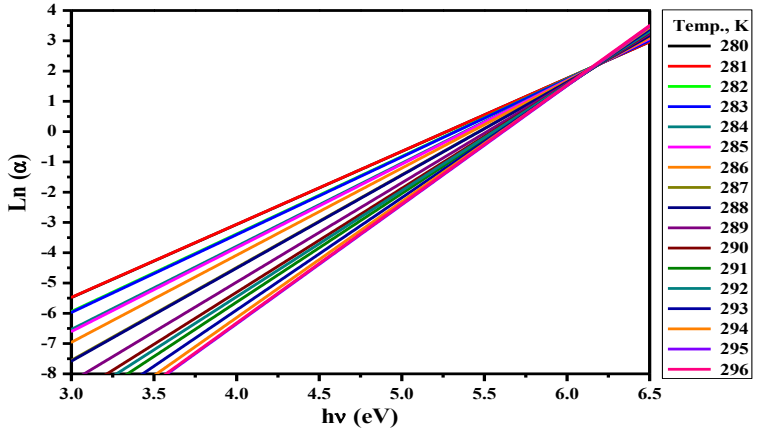

(**ii**)

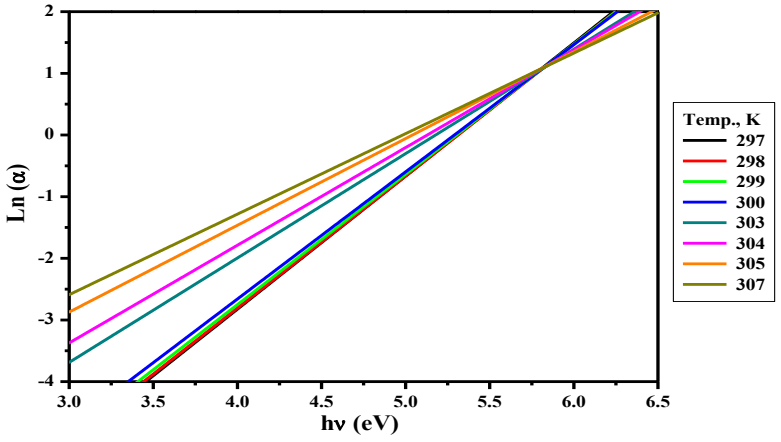

(**iii**)

Fig. (6). Relation between Ln (α) and photon energy (hν) at different temperatures for $(TMA)_2ZnCl_4$ single crystal (**i**) around the commensurate ferroelectric (CF) region (**ii**) around the incommensurate (C) region (**iii**) around the normal paraelectric (N) region.

ly proportional to the strength of the electron-phonon interaction (g) by the relationship [23]:

$$g = \frac{2}{3\ \sigma_o} \tag{7}$$

Values of g for $(TMA)_2ZnCl_4$ crystals for incommensurate (IC) and commensurate (CF) phases are listed in Table **3**. The obtained data show that as the crystal undergoes phase transition a reduction occurs in the value of the coupling constant, and increase in the value of g after transition

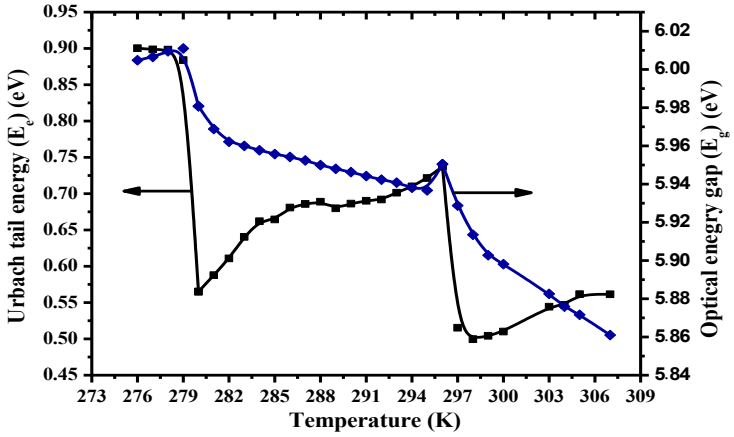

(**i**)

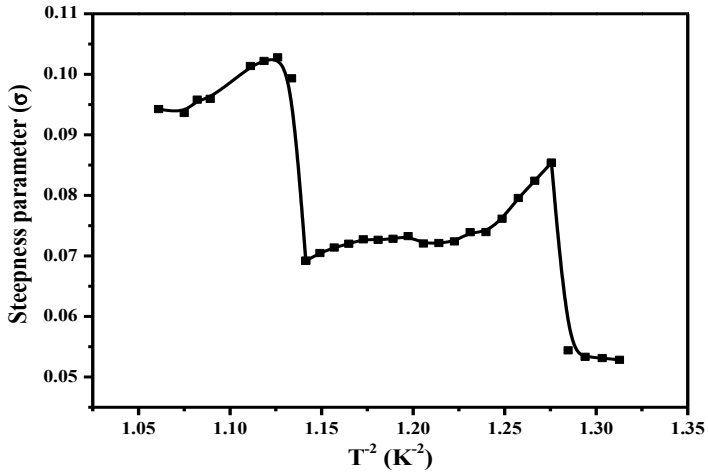

(**ii**)

Fig. (7). (**i**) comparison between width of localized states (E_e) and optical energy gap (E_g) (**ii**) Steepness parameter (σ) versus $1/T^2$ for $(TMA)_2ZnCl_4$ single crystal around the normal-incommensurate-commensurate phases.

which is an evidence of an increase in the degree of ionicity of the crystal bonds. Also there is a change in the electron-phonon interaction constant that may be attributed to a change in the ionicity because of modifications of crystallographic bonds, which occur at phase transition.

After developing $\tanh(\frac{h\nu_o}{2k_BT})$ in a power series of $(\frac{h\nu_o}{2k_BT})$ and ignoring all terms after the second term being very small, it will be possible to determine the steepness parameter and the energy of the participating optical phonons from equation (6). The following equation is the result:

$$\sigma = \sigma_o \left[1 - \frac{1}{3}\left(\frac{h\nu_o}{2k_BT}\right)^2\right] \quad (8)$$

Which indicates a dependence of σ on quadratic temperature. In Fig. (**7-ii**), values of σ are plotted with the corresponding values of $1/T^2$. This figure shows that, the steepness parameter (σ) have a drastic drop at $1/T^2$ equal to 1.285 and 1.141 which corresponds to the temperatures 279 and 296 K, respectively. This anomalous behavior is similar to that observed at the same temperatures in the E_g versus T relationship (Fig. **5-i**).

By linear extrapolation from the low temperature side the paraelectric region, (IC) region and commensurate-ferroelectric (CF), one can obtain the frequency of phonons participating in optical absorption (ν_o) and the value of the electron-optical-phonon coupling constant (σ_o). These values are listed in Table **3**.

Table **3** shows that Urbach parameters are changing with crystal going from the normal to the incommensurate and to the commensurate-ferroelectric phases. The frequency ν_o of the phonons which interact most strongly in the absorption process drastically changes with the phase transition. The change in the electron-phonon interaction constant (σ_o) may be attributed to a change in the ionicity because of modifications of crystallochemical bonds. The absorption tail and the steepness coefficient exhibit a discontinuous and drastic change at the phase transition temperatures. This result indicates that the phase transition influence the Urbach parameters.

3.6. Temperature Dependence of the Absorption Edge

The temperature dependence of the absorption edge for $(TMA)_2ZnCl_4$ crystals plotted in Fig. (**5-i**). From this figure two remarks could be drawn. The first is the anomalies at the paraelectric to incommensurate phase transition temperature (~296 K) and from incommensurate to commensurate-ferroelectric phase transition temperature (~279 K). The anomalous behavior may be due to a change in the electron-phonon interaction at phase transition. The second remark is the linear dependence of E_g with T in both the paraelectric, incommensurate and commensurate phases.

A relation for the variation of the optical energy gap (E_g) with temperature (T) in semiconductors and insulators was proposed [24]:

$$E_g = E_{go} - AT^2(T + D) \quad (9)$$

Where E_{go} is the energy gap value at 0 K, A and D are constants. Most of the variation in the energy gap with temperature may be explained with two mechanisms. The first is a shift in the relative position of the conduction and valence bands due to the temperature dependent dilation lattice [25, 26]. At high temperatures theoretical calculations [26] show that the effect is linear with temperature. In this region, this effect explains only a fraction (about 0.25) of the total variation of the energy gap with temperature. At low temperatures the thermal expansion coefficient is nonlinear with temperatures, for some diamond structure solids it becomes negative [27] over a certain temperature interval. Correspondingly, the dilations effect on the energy gap is also nonlinear. The second mechanism is that the major contribution comes from a shift in the relative position of the conduction and valence bands due to a temperature dependent electron lattice interaction.

In the commensurate-ferroelectric (CF), incommensurate (IC) and paraelectric (PE) or normal (N) phases, E_g varies linearly with temperature. The temperature coefficients of the optical energy gap ($\beta = dE_g/dT$) are calculated in the three phases and they have the values of ($2.1x10^{-3}$ eV/K), ($-2x10^{-3}$ eV/K) and ($-5.3x10^{-3}$ eV/K) respectively. Due to the negative sign of β in the (IC) and (N) phases, the optical energy gap shifts towards the lower energy side with increasing temperature. This variation comes from a shift in the relative positions of the valence and conduction bands due to a temperature dependent of electron lattice interaction [28]. A small fraction of the total variation of the energy gap may be attributed to a shift in the relative position of the valence and conduction bands due to the temperature dependence of the lattice dilation. Because of $\beta_{CF} > \beta_{IC} > \beta_{PE}$, the optical energy gap (E_g) varies with temperature in the paraelectric (PE) or normal (N) phase by a faster rate than the rate in the other two phases.

CONCLUSION

Pure $[N(CH_3)_4]_2ZnCl_4$ single crystals with the dimension of $25 \times 15 \times 8$ mm^3 were grown from aqueous solutions by isothermal evaporation method. The powder X-ray diffraction study confirms the lattice parameter values. It has been found that the optical energy gap studied through the optical properties of high-quality large bulk $(TMA)_2ZnCl_4$ single crystals is temperature dependent. The dependence of the absorption coefficient on the photon energy and on the temperature near the absorption edge obeys the band theory with an exponent referring to the indirect allowed transition is the most probable type of transition. The linear dependence of the optical energy gap on temperature revealed anomalous behavior at the edge in the vicinity of the IC and CF phase transitions. The absorption coefficient exhibited exponential dependence on photon energy following Urbach's rule. The characteristic Urbach parameters were determined. Drastic changes of the parameters at the IC and CF phases were detected.

The following conclusions and possible applications can be listed:

- The results obtained in this study indicate that $(TMA)_2ZnCl_4$ crystal is suitable for optoelectronic applications around room temperature.
- Below T_i this crystal has also the ability of data and optical storage of information directly.
- $(TMA)_2ZnCl_4$ crystal is conveniently transparent in the visible light region with low absorption coefficient in this region which make it suitable for antireflection layers of solar thermal devices and nonlinear optical applications.
- The optical properties of these crystals showed that the optical spectra vary with the temperature. The result of this, for example, is the thermo chromic effect. A very useful practical application is the wireless temperature sensors.

CONFLICT OF INTEREST

The authors confirm that this article content has no conflict of interest.

ACKNOWLEDGEMENTS

Declared None.

REFERENCES

[1] Suchańska M, Kałuża S, Leśniewski S. Some aspects of using A_2MX_2 crystals with incommensurate phases in digital recording. Opto-Electron Rev 2001; 9: 353-5.

[2] Folca CL, Pérez-Mato JM, Tello MJ. Thermal history and dielectric behavior of $[N(CH_3)_4]_2ZnCl_4$ at the incommensurate-commensurate phase transition. Solid State commun 1990; 74: 717-20.

[3] Shmyt'ko IM, Bagautdinov BS. Defect density waves and specific manifestations of the memory effect in crystals with incommensurate phases. Crystallogr Rep 1998; 43: 631-9. (Translated from Kristallografiya 1998; 43: 680-87.

[4] Cho YC, Yoon KH, Hwang YH, Cho CR, Jeong SY. Effects of discommensurations in the C-IC transition of $[N(CH_3)_4]_2ZnCl_4$. J Korean Phys Soc 2002; 41: 381-5.

[5] Gladkii VV, Kirikov VA. Polarization kinetics of a ferroelectric with complex modulated structure. JETP Lett 1999; 70: 42-7.

[6] Lim AR, Jung WK. Proton magnetic resonance study of the phase transitions of $[N(CH_3)_4]_2BCl_4$ (B= ^{59}Co, ^{63}Cu, ^{67}Zn, and ^{113}Cd) single crystals. J Phys Chem Solids 2005; 66: 1795-800.

[7] Wiesner JR, Srivastava RC, Kennard CHL, Di Vaira M, Lingafelter EC. The crystal structures of tetramethylammonium tetrachloro-

cobaltate(II), -nickelate(II), and -zincate(II). Acta Crystallogr 1967; 23: 565-74.

[8] Curtiss ABS, Musie GT, Powell DR. Bis(tetramethylammonium) tetra-chloridozincate(II), phase VI. Acta Crystallogr 2008; E64: m183.

[9] Hong Le, Li Gen, Tao N, Cummins H. Critical slowing down of low-frequency dielectric relaxation in incommensurate $[N(CH_3)_4]_2ZnCl_4$. Phys Rev B 1990; 41: 6050-6.

[10] Sveleba S, Katerynchuk I, Kunyo I, Karpa I, Semotyuk O, Czapla Z. Birefringent and dielectric properties of $[N(CH_3)_4]_2ZnCl_4$ in parent phase. J Phys 2008; 53: 1098-100.

[11] Vlokh OG. Parametric crystal optics of nonmagnetic ferroics. Condens Matter Phys 1998; 1: 339-56.

[12] Sawada S, Yamaguichi T, Suzuki H, Shimizu F. Experimental studies on phase transitions in ferroelectric $\{N(CH_3)_4\}_2ZnCl_4$. J Phys Soc Jpn 1985; 54: 3129-35.

[13] Abu El-Fadl A, El-Korashy A, El-Zahed H. Electrical investigations in the normal and incommensurate phases of $[N(CH_3)_4]_2ZnCl_4$ single crystals. J Phys Chem Solids 2002; 63: 375-81.

[14] Sveleba SA, Katerinchuk IM, Semotyuk OV, *et al.* Temperature dependence of the crystal-optics characteristics of $[N(CH_3)_4]_2ZnCl_4:Ni^{2+}$ crystals with correlated motion of tetrahedral groups. Crystallography Reports 2010; 55: 253-7.

[15] Aleksandrov KS, Beznosikov BV. Phase transitions in crystals related to α-K_2SO_4. Ferroelectrics 1991; 117: 331–45.

[16] El-Korashy A. Optical band gap studies of $[N(CH_3)_4]_2ZnCl_4$ single crystals on the paraelectric phase. J Mater Sci Lett 2000; 19: 29-31.

[17] El-Korashy A, El-Zahed H, Radwan M. Optical studies of $[N(CH_3)_4]_2CoCl_4$, $[N(CH_3)_4]_2MnCl_4$ single crystals in the normal paraelectric phase. Physica B 2003; 334: 75-81.

[18] Martienssen W. Über die excitonenbanden der alkalihalogenidkristalle. J Phys Chem Solids 1957; 2: 257-67.

[19] Urbach F. The long-wavelength edge of photographic sensitivity and of the electronic absorption of solids. Phys Rev 1953; 92: 1324.

[20] Kruik MV. Urbach rule. Phys Stat Sol a 1971; 8: 9-45.

[21] Pačesová S, Březina B, Jastrabík L. Optical properties of K_2SeO_4 in the vicinity of phase transitions. Phys Stat Sol b 1983; 116: 645-52.

[22] Mahr H. Ultraviolet absorption of ki diluted in KCl crystals. Phys Rev 1962; 125: 1510-6.

[23] Dunja I, Kranycec M, Celustka B. Optical absorption edge and Urbach's rule in mixed single crystals of $(Ga_xIn_{1-x})_2Se_3$ in the indium rich region. J Phys Chem Solids 1991; 52: 915-20.

[24] Varshni VP. Temperature dependence of the energy gap in semiconductors. Physica 1967; 34: 149-54.

[25] Möglich F, Rompe R. Über den Einfluß Der wärmedehnung Auf Das Absorptionsspektrum Von Isolatoren. Z Phys 1942; 119: 472-81.

[26] Bardeen J, Shockley W. Deformation potentials and mobilities in non-polar crystals. Phys Rev 1950; 80: 72-80.

[27] Collins JG, White GK. Chapter IX: thermal expansion of solids. In: Gorter CJ, Ed, progress in low temperature physics, 1964; 4: 450-79.

[28] Muto T, Ôyama S. Theory of the temperature effect of electronic energy bands in crystals. Prog Theory Phys 1950; 5: 833-43.

Received: March 28, 2015 Revised: June 17, 2015 Accepted: July 08, 2015